Supplementary information to:

Deposition nucleation on mineral dust particles: a case against classical nucleation theory with the assumption of a single contact angle

M. J. Wheeler and A. K. Bertram

Department of Chemistry, University of British Columbia,
Vancouver, BC V6T 1Z1, Canada

We have performed an additional series of calculations to asses the sensitivity of the results in the main document to the assumption of spherical particles. In the main text we assumed the surface area of a particle was equal to the geometric surface area (i.e. the particles are spherical). Here we reanalyze the results with the assumption that the surface area equals the geometric surface area multiplied by 50, as an upper limit to the surface area.

Table S1: Fit parameters obtained for kaolinite assuming the surface area equals the geometric surface area multiplied by 50. Best fits were obtained by minimizing the weighted residual sum of squares between the experimental data and the fit function.

Model	Parameter	Value	RSS[a]
Single-α	α	$19.76°$	15.771
PDF-α	$\bar{\alpha}$	$0°$	3.919
	σ_α	$55.29°$	
Active site	b	$7.4 \times 10^7 \mathrm{m}^{-2}$	5.492
	β_1	0.01	
	β_2	0.001	
Deterministic	A_1	$2.39 \times 10^4 \mathrm{cm}^{-2}$	0.541
	A_2	-0.8547	

[a] Residual sum of squares

Table S2: Fit parameters obtained for illite assuming the surface area equals the geometric surface area multiplied by 50. Best fits were obtained by minimizing the weighted residual sum of squares between the experimental data and the fit function.

Model	Parameter	Value	RSS[a]
Single-α	α	$22.21°$	9.798
PDF-α	$\bar{\alpha}$	$36.13°$	0.0371
	σ_α	$14.91°$	
Active site	b	$1.5 \times 10^8 \mathrm{m}^{-2}$	0.754
	β_1	0.1367	
	β_2	1.0×10^{-4}	
Deterministic	A_1	$2.93 \times 10^4 \mathrm{cm}^{-2}$	0.00783
	A_2	-0.9415	

[a] Residual sum of squares

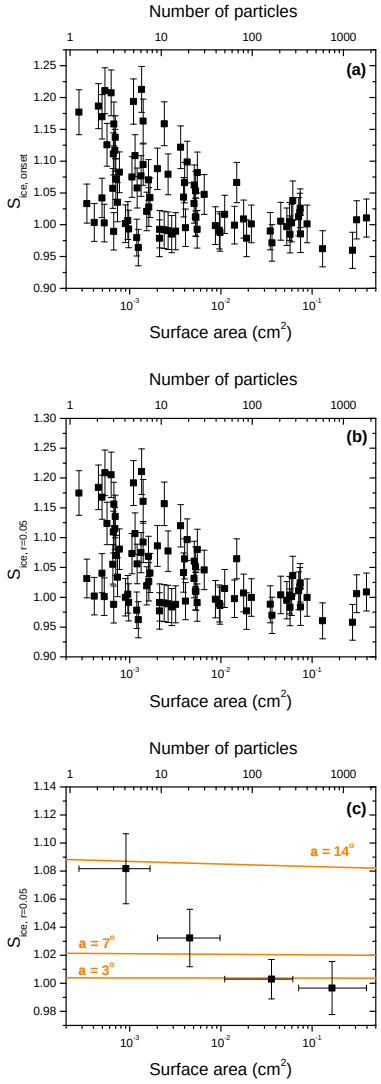

Figure S1: Results for kaolinite particles: **(a)** individual onset measurements, **(b)** individual $S_{\mathrm{ice,\,r=0.05}}$ results and **(c)** average $S_{\mathrm{ice,\,r=0.05}}$. The average values are calculated for four equally sized bins and the horizontal error bars show the range of data points in each bin. The surface area values in **(c)** represent the average surface area of the points in each bin. Error in $S_{\mathrm{ice,\,onset}}$ is given as experimental error in measurements of saturation. Error in $S_{\mathrm{ice,\,r=0.05}}$ is based on the difference between $S_{\mathrm{ice,\,onset}}$ and $S_{\mathrm{ice,\,previous}}$ as well as the uncertainty in measuring $S_{\mathrm{ice,\,onset}}$. Error in the average $S_{\mathrm{ice,\,r=0.05}}$ represents the 95 % confidence interval. Predictions are shown using the single-α model (orange lines) calculated using Eq. (9). In addition to surface area, the corresponding number of particles calculated from A_{average} is also shown. The surface area was assumed to be the geometric surface area multiplied by a factor of 50.

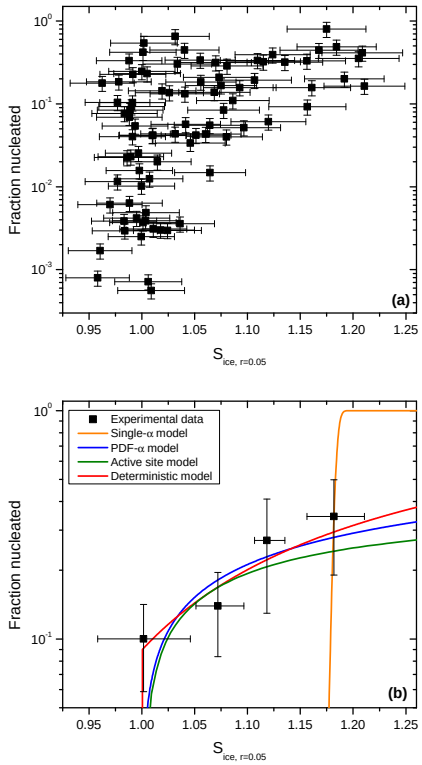

Figure S2: Fraction of particles nucleated as a function of $S_{\mathrm{ice,\,r=0.05}}$ for kaolinite. Panel **(a)** shows nucleated fraction for the individual experimental results. The y-error was calculated from the uncertainty in the value of $\bar{D_g}$. The x-error represents the uncertainty in $S_{\mathrm{ice,\,r=0.05}}$. Panel **(b)** shows the average nucleated fraction calculated for four size bins. The range of the data points in each bin is given as the horizontal error and data points represent the average of the $S_{\mathrm{ice,\,r=0.05}}$ values within each bin. The y-error bar in panel **(b)** represents the 95 % confidence interval of the average nucleated fraction. Fits are shown for the single-α, PDF-α, active site, and deterministic models. The surface area was assumed to be the geometric surface area multiplied by a factor of 50.

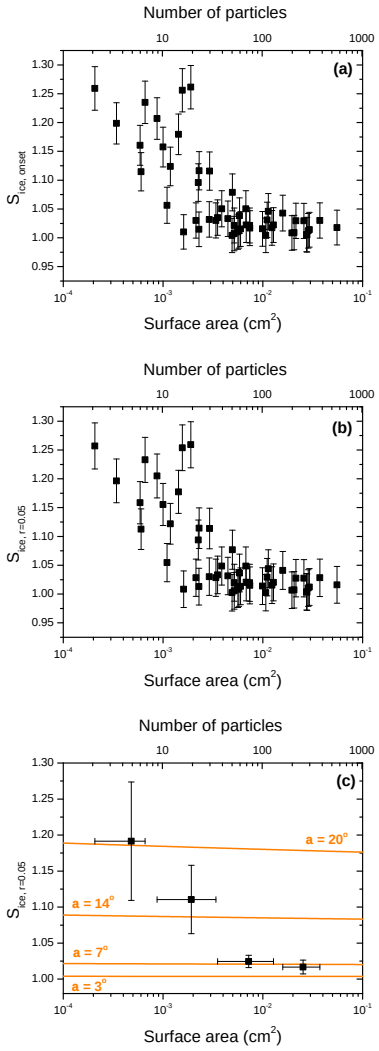

Figure S3: Results for illite particles: **(a)** individual onset measurements, **(b)** individual $S_{\mathrm{ice,\,r=0.05}}$ results and **(c)** average $S_{\mathrm{ice,\,r=0.05}}$. The average values are calculated for four equally sized bins and the horizontal error bars show the range of data points in each bin. The surface area values in **(c)** represent the average surface area of the points in each bin. Error in $S_{\mathrm{ice,\,onset}}$ is given as experimental error in measurements of saturation. Error in $S_{\mathrm{ice,\,r=0.05}}$ is based on the difference between $S_{\mathrm{ice,\,onset}}$ and $S_{\mathrm{ice,\,previous}}$ as well as the uncertainty in measuring $S_{\mathrm{ice,\,onset}}$. Error in the average $S_{\mathrm{ice,\,r=0.05}}$ represents the 95 % confidence interval. Predictions are shown using the single-α model (orange lines) calculated using Eq. (9). In addition to surface area, the corresponding number of particles calculated from A_{average} is also shown. The surface area was assumed to be the geometric surface area multiplied by a factor of 50.

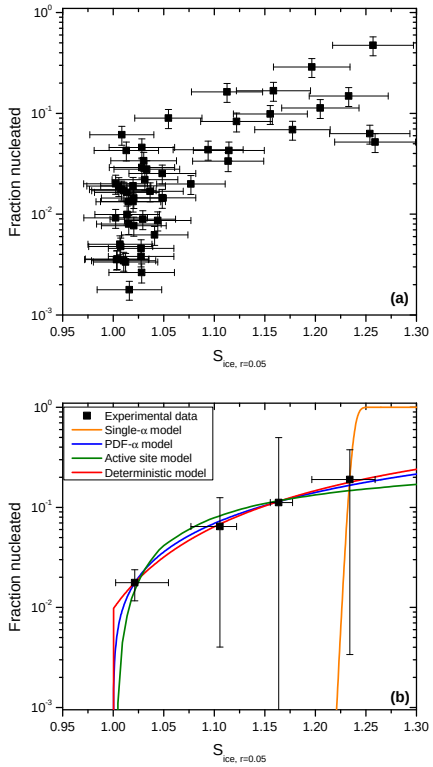

Figure S4: Fraction of particles nucleated as a function of $S_{\mathrm{ice,\,r=0.05}}$ for illite. Panel **(a)** shows nucleated fraction for the individual experimental results. The y-error was calculated from the uncertainty in the value of $\bar{D_g}$. The x-error represents the uncertainty in $S_{\mathrm{ice,\,r=0.05}}$. Panel **(b)** shows the average nucleated fraction calculated for four size bins. The range of the data points in each bin is given as the horizontal error and data points represent the average of the $S_{\mathrm{ice,\,r=0.05}}$ values within each bin. The y-error bar in panel **(b)** represents the 95 % confidence interval of the average nucleated fraction. Fits are shown for the single-α, PDF-α, active site, and deterministic models. The surface area was assumed to be the geometric surface area multiplied by a factor of 50.